Application of Laskin fractional quantum mechanics with a changed fractional differential operator to one-dimensional potentials

L. Y. Medina and J. D. Correa

Facultad de Ciencias Básicas, Universidad de Medellín, Medellín, Colombia,
e-mail: jcorrea@udemedellin.edu.co

M. E. Mora-Ramos

Centro de Investigación en Ciencias-IICBA. Universidad Autónoma del Estado de Morelos,
Av. Universidad 1001, CP 62209, Cuernavaca, Morelos, Mexico,
e-mail memora@uaem.mx

J. F. Pérez-Torres

Escuela de Química, Universidad Industrial de Santander, Bucaramanga, Colombia.

Received 30 April 2024; accepted 2 September 2024

We studied the quantum mechanics problem of certain one-dimensional potential functions using Laskin fractional quantum mechanics. We used different representations to describe the kinetic energy operator, including the conformable and Riemann-Liouville-Caputo fractional differential operators. We then compared each approach's energy states and wave function outcomes for single and double rectangular and harmonic potentials. As the fractional index increased, there was a noticeable difference between the excited energy values resulting from each method. When the system exhibits degeneracy, we find noticeable changes in the probability densities. Our results provide a straightforward and standardized approach for solving the one-dimensional fractional Schrödinger equation numerically.

Keywords: Fractional quantum mechanics; 1D problems; Riemann-Liouville-Caputo formulation; conformable formulation.

DOI: https://doi.org/10.31349/RevMexFis.71.020703

1. Introduction

Fractional calculus is a fascinating and relatively unexplored branch of mathematics that extends the concepts of differentiation and integration to non-integer orders. While classical calculus deals with whole numbers as exponents, fractional calculus allows to work with real or complex numbers as exponents in the involved operators, providing a powerful mathematical framework to describe and analyze a wide range of natural phenomena and engineering processes [1]. Throughout history, fractional calculus has had intermittent periods of interest and obscurity. Early pioneers such as Leibnitz (on a question posed to him by L'Hôpital), Bernoulli, Euler, and Laplace initially dealt with the subject. However, it was until 19th century that renowned mathematicians like Liouville and Riemann began to formalize the theory.

Interest in fractional calculus has been resurgent in recent times due to its relevance in modeling complex systems and phenomena. For instance, over the past few decades, a unique approach to exploring the fundamental principles of physics has emerged: The inception of fractional quantum mechanics. It can be traced back to 2000-2002, when N. Laskin employed fractional calculus to derive a modified version of the Schrödinger equation [2,3]. This modification arose from his previous work on the application of fractal principles to the description of path integrals for Lévy flight trajectories (see Ref. [4]) which implies a restriction for the values of Lévy's index to lie within the interval $[1, 2]$. As a follow up, Laskin's work, incorporating the quantum Riesz fractional derivative, extended conventional quantum mechanics into a fractional counterpart. The resulting Schrödinger equation with fractional Hamiltonian is, in general form:

$$i\hbar\partial_t\Psi(x,t) = \hat{H}_\alpha\Psi(x,t), \tag{1}$$

with

$$\hat{H}_\alpha = \mathcal{D}_\alpha D^\alpha + V(\hat{x},t). \tag{2}$$

In Laskin's formulation, the particular case with Lévy's index $\alpha = 2$, having $D_2 = \hbar/2m$, represents the conventional formalism (see Eq. (30) in Ref. [4]). This indicates that fractional quantum mechanics encompasses conventional one as the particular situation having the upper limit of Lévy's index values. In other words, the nature or explanation of the presence of a fractional derivative in the Schrödinger equation lies, precisely, on α-index, and can be interpreted as leading to a free-particle dispersion relation of the form $E(k) = E_0 k^\alpha$, which becomes a fractional generalization of the dispersion relation $E(k) = E_0 k^2$ corresponding to D'Broglie waves.

However, there has been a scarcity of methods for the analytical solution of fractional Schrödinger equation as proposed by Laskin. As a particular example, we can mention the solutions to space fractional Schrödinger equation using momentum representation method [5]. Actually, numerical approaches are more common. A quite recent example is the report of Medina and coworkers on the application of

fractional Fourier grid Hamiltonian method to the study of molecular vibrations in H_2 and D_2, described with the use of quantum Riesz fractional momentum operator [6].

Applications of fractional calculus to physics problems have been put forward, mainly after the introduction of *conformable fractional derivation* by Khalil *et al*. in 2014 [7]. In that sense, fractional Newton mechanics was developed [8]. With the introduction of a fractional version of the calculus of variations and the construction of fractional Euler-Lagrange equations, some one-dimensional (1D) mechanical examples were solved. On the other hand, multivariable conformable calculus was applied to modeling physical oceanographic phenomena [9]. Quantum mechanical problems have also been dealt with. Schrödinger and Dirac 1D harmonic oscillator, and their thermal properties, were investigated using Riesz fractional derivative [10]. Conformable approach was applied in the case of the formation of quantum-mechanical operators [11], and to derive a solution for the angular part fractional Schrödinger equation [12].

The 1D quantum wells (1DQWs) are one of the most studied quantum mechanical problems. They are obligatory problems to solve in elementary quantum mechanical courses because they offer not only the possibility of studying the Schrödinger equation analytically but the efficient implementation of numerical solutions. Beyond this, 1DQW models are employed to study the physical properties of systems where quasi-two-dimensional carrier confining structures can be formed when two large band gap semiconductor layers sandwich another semiconductor layer with smaller band gap; thus making possible to fabricate optoelectronic devices such as photo-detectors, lasers, sensors, and quantum modulators [13]. These semiconductor layers could be assembled by modern crystal growth means like molecular beam epitaxy (MBE) [14]. In addition, quantum wells with one-dimensional confinement are extensively used in modern electronic devices.

In this work, we are aimed at presenting the solution of some of the simplest 1D problems of quantum mechanics, described by the time-independent Schrödinger fractional operator. Some of these solutions will be determined via a numerical treatment based on suitable generalized Fourier expansions. The Riemann-Liouville (RLC) and the conformable representations are used to describe the fractional kinetic energy operator, and the outcomes from both approaches are compared in each case. These solutions could open the way to explaining phenomenological effects as compressive strains or effective crystalline potential that regularly are explained employing the effective mass approximation. The article is organized as follows: In Sec. 2 we briefly define the fractional derivatives considered. Next, the quantum equation of work is introduced and the method for its approximate solution is presented. Section 4 contains the results for the considered problems and, finally, conclusions are given.

2. Defining fractional derivative

Fractional calculus is a branch of Mathematics which generalizes the traditional concept on function derivation. As mentioned, since its beginnings several definitions of fractional derivatives have been formulated. Here, we are going to deal with two examples.

2.1. Riemann-Liouville-Caputo

This definition was separately given by J. Liouville and B. Riemann in the first half of 19th. century. It is provided on the basis of an integral operator, J:

Definition 1. *L*et $n \in \mathbb{R}^+$, be the operator J_α^n defined in the space $L_1[a,b]$ by:

$$J_{(a)}^n f(x) = \frac{1}{\Gamma(n)} \int_a^x (x-t)^{n-1} f(t) dt, \tag{3}$$

for $a \leq x \leq b$, it is called the Riemann-Liouville integral operator of order n.

Then, the fractional Riemann-Liouville definition of derivation has the form: $D^\alpha f(t) = D^m J^{m-\alpha} f(t)$, where $m-1 < \alpha < m$, and $m \in \mathbb{Z}^+$. Then for a continuous funtion one finds,

$$D^\alpha f(t) = \frac{1}{\Gamma(m-\alpha)} \frac{d^m}{dt^m} \left[\int_0^t \frac{f(\tau)}{(t-\tau)^{\alpha+1-m}} d\tau \right]. \tag{4}$$

It is relevant commenting that, in 1967, Italian mathematician M. Caputo proposed an alternative definition (from hereon labeled as RLC) of Riemann-Liuoville fractional derivation which, among other things, produces the zero value when f is a constant. In terms of the -non-commutable- differential and integral operators, we have $D^\alpha f(t) = J^{m-\alpha} D^m f(t)$, where $m-1 < \alpha < m$, and $m \in \mathbb{Z}+$, leading to

$$D_C^\alpha f(t) = \frac{1}{\Gamma(m-\alpha)} \int_0^t \frac{f^{(m)}(\tau)}{(t-\tau)^{\alpha+1-m}} d\tau. \tag{5}$$

The latter, RLC, expression is the one we shall employ in the present work.

2.2. Conformable

Much more recently, in 2014, Khalil and collaborators introduced what seems to be a more "natural" definition of fractional derivation, in the sense that no integral operator is involved. They named it as "conformable" [7] and, for $0 \leq \alpha < 1$, it coincides with -up to a constant- the classical definitions over polynomials. Let $f : [0, \infty] \longrightarrow \mathbb{R}$. Then, its conformable fractional derivative of α-th order is obtained from,

$$T_\alpha(f)(t) = \lim_{\varepsilon \to 0} \frac{f(t + \varepsilon t^{1-\alpha}) - f(t)}{\varepsilon}, \tag{6}$$

for all $t > 0$, $\alpha \in (0,1)$. If f is differentiable in some $(0,a), a > 0$ and $\lim_{t \to 0^+} f^{(\alpha)}(t)$ exists, then it is defined: $f^{(\alpha)}(0) = \lim_{t \to 0^+} f^{(\alpha)}(t)$. It holds the following

Theorem 1. *Let $\alpha \in (0,1]$ and f, $\alpha-$differentiable in a point $t>0$, then* $T_\alpha(f)(t) = t^{1-\alpha}(df/dt)(t)$.

3. Fractional Schrödinger equation. The expansion method

Now, we assume that the fractional Hamiltonian operator in Eq. (2) is time-independent. In consequence, it is only needed to solve the corresponding stationary Schrödinger equation

$$-\mathcal{D}_\alpha D^{2\alpha}\psi(x) + \tilde{V}(x)\psi(x) = \tilde{E}\psi(x), \tag{7}$$

where $\mathcal{D}_\alpha = (\hbar^{2\alpha}/2m)(mc)^{2-2\alpha}$, with $0 < \alpha \leq 1$, is the diffusion coefficient [15]. Here c is the speed of light in vacuum. Equation (7) can be put in a dimensionless form by using fractional Rydberg, Ry_α, as energy unit and fractional Bohr radius, a_0, as unit of length (for the definition of fractional atomic units see Appendix A):

$$-\frac{1}{2\alpha-1}D^{2\alpha}\psi(x) + \tilde{V}(x)\psi(x) = \tilde{E}\psi(x). \tag{8}$$

It is worth commenting at this point that the process of transforming the fractional Schrödinger equation into a dimensionless expression, using fractional atomic units, transforms the potential energy term into a fractional one as well; since it becomes dependent on α through the effective Rydberg: $\tilde{V} = V/Ry_\alpha$.

3.1. The example of a single one-dimensional quantum well

As a first example, we shall present the analytical solution of the fractional quantum mechanical problem of a finite barrier one-dimensional potential well of effective width l:

$$\tilde{V}(x) = \begin{cases} 0, & \text{if} \quad x \in [0,l], \\ \tilde{v}_o, & \text{if} \quad x \notin [0,l]. \end{cases} \tag{9}$$

This is one of the simplest situations discussed in quantum mechanics textbooks. It is worth commenting at this point that the model potentials used here are not intended to reflect specific real situations, but only to serve as examples for numerical comparisons. So, by taking advantage of the simpler algebraic structure of conformable derivative, it is possible to reach analytical solutions. Within the formulation put forward by Khalil *et al.* the definition of conformable derivative assumes positive values of the coordinate [7]. However, Chung *et al*. extend the definition to include negative values through the incorporation of the factor $|x|^{1-\alpha}$ instead of solely $x^{1-\alpha}$, keeping the same general properties of the conformable approach [11]. In that sense, we are choosing the active region of the quantum well in Eq. (9) to be in the real semi-axis. Accordingly, the general solution for the wavefunctions can be written as:

$$\psi(x) = \begin{cases} Ce^{-\frac{k_2}{\alpha}|x|^\alpha}, & x < 0, \\ A\sin(\frac{k_1}{\alpha}x^\alpha) + B\cos(\frac{k_1}{\alpha}x^\alpha) & x \in [0,l], \\ De^{-\frac{k_2}{\alpha}x^\alpha}, & x > l, \end{cases} \tag{10}$$

where $k_1 = \sqrt{(2\alpha-1)\widetilde{E}}$ and $k_2 = \sqrt{(2\alpha-1)(\tilde{v}_o - \widetilde{E})}$, and $\tilde{E}$ is the effective energy. The corresponding transcendent equation for the allowed energy levels results from equating to zero the determinant of the system of equations for $A\,, B\,, C\,, D$ arising from imposing continuity of $\psi(x)$ and $D^\alpha\psi(x)$ at $x=0$ and $x=l$:

$$\tan\left(\frac{k_1 l^\alpha}{\alpha}\right) = \frac{2k_1k_2}{k_1^2 - k_2^2}. \tag{11}$$

Clearly, Eq. (11) needs to be solved numerically in order to obtain the energies of bound states in the problem. However, in what follows, we shall proceed in a different way. Since we are interested in making a comparison between conformable and RLC formalisms, the numerical solving will be carried out for both formulations by means of the expansion method. In what follows, we give a more detailed explanation of this approach.

3.1.1. Diagonalization method

This scheme of calculation, also named as diagonalization method, relies on proposing the solution of the fractional Schrödinger problem in the form of a Fourier-type expansion over a suitable normalized basis, $\{\phi_n(x)\}$, in the Hilbert space:

$$\psi(x) = \sum_{n=0}^{N} C_n\phi_n(x). \tag{12}$$

Then, with the substitution of (12) in the equation of motion (8), a Hamiltonian matrix is constructed. Its diagonalization, leads to the system energy eigenvalues. In our case, for the sake of simplicity, the building of an expansion basis uses the corresponding solutions of an infinite rectangular quantum well within each of the considered formulations. To guarantee compliance with original conformable formulation of Ref. [7], the finite barrier quantum well as well as the infinite barrier one are assumed to lie well within the positive real axis. For the sake of brevity in main text of this article, full details of the procedure are presented in Appendix B.

Numerical solution for the 1D finite barrier single quantum well using this approach produces the results presented in Fig. 1 for the allowed energy levels. In the calculation, well width is set as $l = 2\,$nm and the potential well depth is $v_0 = 30$ eV. Moreover, the outer infinite barrier used to construct the basis is $L = 10l$, and the total number of terms in the expansion -chosen to guarantee proper convergence- is $N = 150$. Variation in the fractional index α occurs within

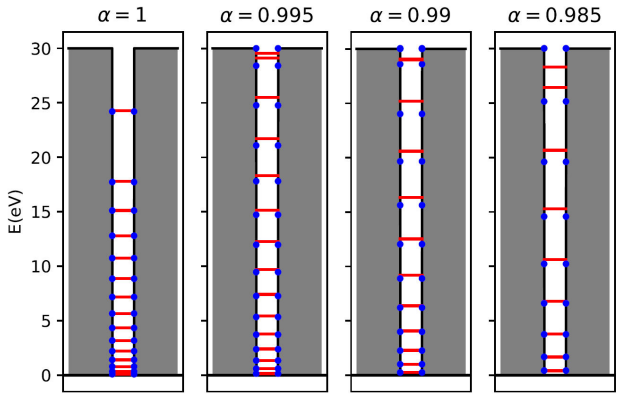

FIGURE 1. Representation of ten first energy states corresponding to 1D finite barrier single quantum well with $l = 2\,\text{nm}$, $v_0 = 30\,\text{eV}$, $N = 150$, and $L = 10l$. Results are for Riemann-Liouville (blue dots) and conformable (red lines) formulations, considering four different values of α.

the range from 1 to 0.985. It can be noticed that, even such a small change leads to significant variations in the energies of the states, compared to the non-fractional situation. In fact, the further decrease in this index causes the number of confined states within the well to diminish. On the other hand, both formulations give quite close values for the ground and first excited states, but energy values obtained from RLC and conformable approaches deviate in a noticeable way for the upper confined states as the fractional index value decreases. Reducing α ultimately leads to the expulsion of levels from the potential well, as can be noticed by observing the Fig. 1. This effect is equivalent to the progressive narrowing of the potential well -with fixed depth- in the non-fractional case. It resembles that occurring in regular 1D Schrödinger problem due to narrowing the well width while keeping its depth.

From the corresponding wavefunction, one may observe that -normalized- ground and first-excited state wavefunctions keep their form independently of the fractional index, α. In Fig. 2 the corresponding probability densities are shown. Actually, it is apparent that, as long as α diminishes, the states become -slightly- less localized within the well region, which is more apparent for the conformable formulation. It is important to note that the wave function is always square-integrable. This points at the possibility of still interpreting squared wavefunction module as the spatial probability of finding a particle, just as in the regular Schrödinger formulation. It is worth bringing attention to the fact that basis functions $\phi_n(x) \sim \sin(n\pi/L^\alpha x)$, chosen for the expansion in conformable case, are orthogonal with a weight $x^{\alpha-1}$ for different values of n-index [11]. So, expansion (15) remains justified within the particular linear space associated to the fractional Hamiltonian operator.

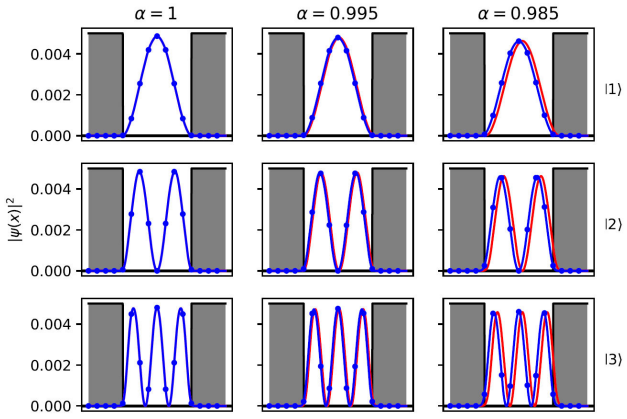

FIGURE 2. Probability densities corresponding to the three lowest confined states of 1D finite barrier single quantum well with $l = 2\,\text{nm}$, $v_o = 30\,\text{eV}$, $N = 300$, $b = l$, and $L = 6l$. Results are for Riemann-Liouville (blue dots) and conformable (red lines) formulations. All wave functions are normalized.

3.2. Finite barrier double quantum well

Let us now analyze the features of the spectrum of confined states in a symmetric, finite barrier, double quantum well. The potential energy profile, having a central barrier of width b, is described as:

$$V(x) = \begin{cases} 0, & \text{if } -\frac{l}{2}-\frac{b}{2} \leq x-d \leq -\frac{b}{2} \quad \text{and} \\ & \frac{b}{2} \leq x-d \leq \frac{l}{2}+\frac{b}{2}, \\ v_o, & \text{if } |x-d| < \frac{b}{2} \text{ and } |x-d| < \frac{l}{2}+\frac{b}{2}. \end{cases} \tag{13}$$

Solutions, in this case, have been determined numerically through the diagonalization process previously commented. The center of the well is chosen to be placed at $x = d$, sufficiently inside the positive real interval, in order to ensure the applicability of the original conformable formulation during the diagonalization process. It is well known that this kind of shifting does not affect at all the results for the energy spectrum. The analysis considers two different widths of the inner central barrier: In Fig. 3 we show a representation of the calculated lowest confined states in a structure with the following configuration: $l = 2\,\text{nm}$, $v_0 = 30\,\text{eV}$, $N = 150$, $b = l/2$, and $L = 10(2l+b)$. Results are plotted for both the RLC and

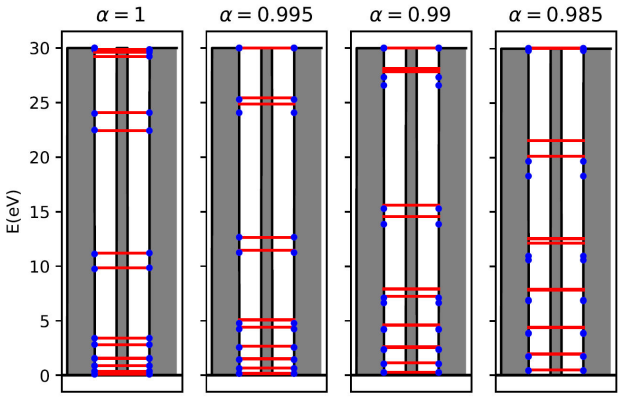

FIGURE 3. Representation of twenty first energy states corresponding to 1D finite barrier double quantum well with $l = 2\,\text{nm}$, $b = l/2$, $v_0 = 30\,\text{eV}$, $N = 150$, and $L = 10(2l+b)$. Results are for Riemann-Liouville (blue dots) and conformable (red lines) formulations, considering four different values of α.

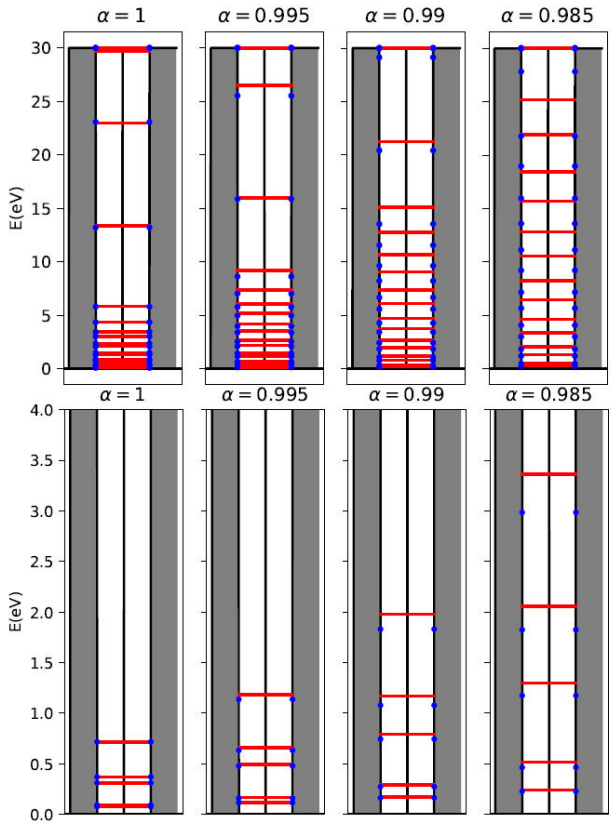

FIGURE 4. Representation of twenty first energy states corresponding to 1D finite barrier double quantum well with $l = 2\,\text{nm}$, $b = l/200$, $v_0 = 30\,\text{eV}$, $N = 150$, and $L = 10(2l + b)$. Results are for Riemann-Liouville (blue dots) and conformable (red lines) formulations, considering four different values of α. Bottom plot shows a zooming of the lower energy region.

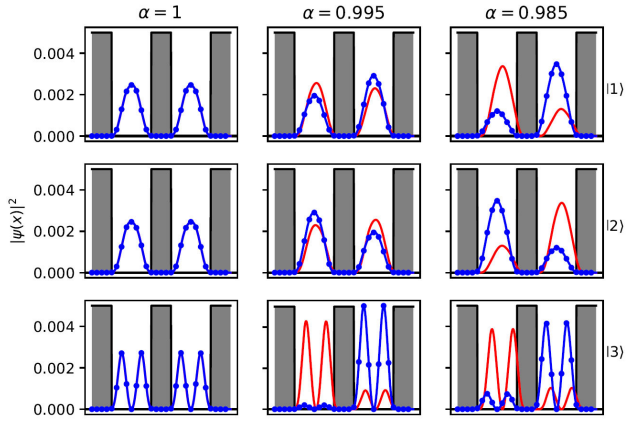

FIGURE 5. Probability densities corresponding to the lowest confined states in a structure with $l = 2\,\text{nm}$, $b = l/200$, $v_0 = 30\,\text{eV}$, $N = 150$, and $L = 10(2l + b)$. Results are for Riemann-Liouville (blue-dotted) and conformable (red-solid) formulations.

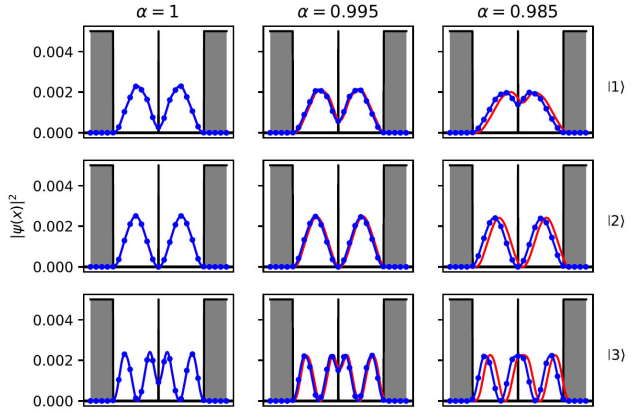

FIGURE 6. Probability densities corresponding to the lowest confined states in a structure with $l = 2\,\text{nm}$, $b = l/2$, $v_0 = 30\,\text{eV}$, $N = 150$, and $L = 10(2l + b)$. Results are for Riemann-Liouville (blue-dotted) and conformable (red-solid) formulations.

conformable formulations of the fractional kinetic operator in the Schrödinger equation. On the other hand, energy values depicted in Fig. 4 correspond to the setup that only differs from the previous one in a more thinner width of inner barrier, $b = l/200$. The lower plot in this figure contains a zoom of the interval of energies between 0 and 5 eV. It allows to better notice the influence of changing the fractional index, α over the spectrum of confined states in the system.

Once again, coincidence of energy state results calculated from both formulations starts to fade away quite quickly even for very small deviations from the non-fractional case. This can be observed even for the ground energy level, but starts being more apparent for the first and second excited ones. Such differences are bigger than in the situation of a single quantum well, discussed above, and enhance as the thickness of central barrier augments. Accordingly, it is possible to notice a real difference between the formulations when effective spatial dimensions of the system are larger. As a curious effect, in double well systems, states located almost at the barrier edge are kept, independently of the α-values considered.

With regard to the probability densities (see Figs. 5 and 6), the most remarkable feature -mainly for the excited states- is the interchange of the maximums of probability with respect to the center of the confining structure. This phenomenon is significantly more notorious in the case of a wider inner barrier. This contrasts with the non-fractional situation, for which all distributions are symmetric. With respect to this feature, it is not difficult to determine that the conformable fractional derivative of any function of real variable lacks of spatial symmetry, provided the presence of the multiplicative term $t^{1-\alpha}$ (see Theorem II.1 above), which readily introduces a complex factor under -for instance- spatial inversion, which not necessarily has unit modulus.

Another notorious fact has to do with the exchange of amplitudes in fractional results. That is, when maximum values of the wavefunctions appear at the right well region in one of the fractional formulations, they localize within the left well region in the other. This is clearly observed in the configuration with a thicker inner barrier. This situation affects the non-symmetric probability density distribution in the problem when it is described within one formulation or the other. Again, the increasing separation between results of

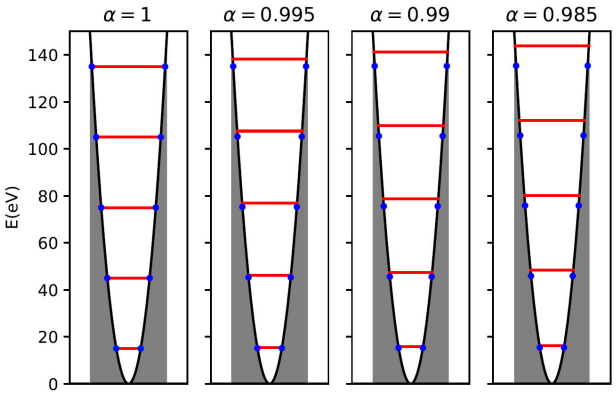

FIGURE 7. Schematic view of fractional quantum harmonic oscillator potential and the corresponding calculated energy values for different values of the fractional index, α. Dots correspond to levels obtained with the Riemann-Liouville-Caputo description and lines correspond to the conformable one.

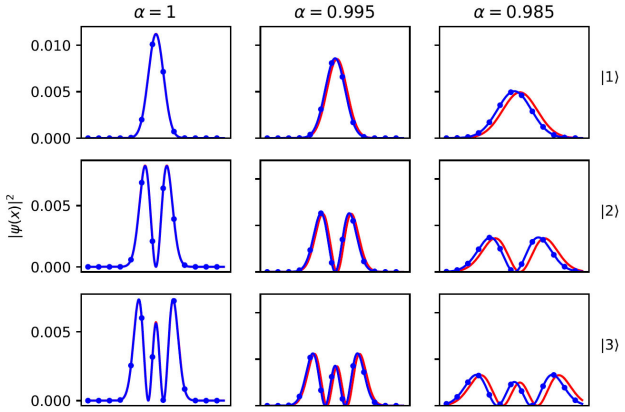

FIGURE 8. Probability densities corresponding to fractional description of a quantum harmonic oscillator potential for different values of the fractional index, α. Results are for Riemann-Liouville (blue-dotted) and conformable (red-solid) formulations.

conformable and RLC descriptions, as long as α increases, are highlighted.

3.3. Fractional harmonic oscillator

The potential energy function in the case of a fractional quantum harmonic oscillator is given by the following expression [3]:

$$V(x) = \frac{1}{2}m\omega^2 \frac{\hbar^2}{2m\mathcal{D}_\alpha}|x|^{2\alpha}. \tag{14}$$

Figure 8 contains a view of the potential profile for a number of values of the fractional index α. It is possible to notice that the symmetric character of $V(x)$, in this case, is kept all the time. The main difference associated with reducing α is the opening of the potential well width.

In previous works, the energy spectrum of the fractional quantum harmonic oscillator has been analytically determined, within the RLC formulation, using the WKB method [3,16]. The obtained expression is the following,

$$E_n = \left(n+\frac{1}{2}\right)^\beta \pi^{\beta/2}\left(\beta\frac{\Gamma\left(\frac{1+\beta}{2\beta}\right)}{\Gamma\left(\frac{1}{2\beta}\right)}\right)^\beta, \tag{15}$$

with $n = 0, 1, 2, ...$ and $2\beta = \alpha$.

By setting $\hbar\omega = 30$ eV, the values of lowest three allowed quantum states in the oscillator problem are presented in Table I. There, together with the RLC-WKB results obtained with Eq. (15), we include the exact non-fractional value ($\alpha = 1$) from the well-known expression $E_n = \hbar\omega(n+1/2)$, together with the output of the diagonalization scheme under conformable formulation, with 500 elements in the expansion base.

In this case, one may also appreciate a difference in the energy values of first and second excited states, obtained from WKB approximation and the diagonalization method. The accuracy of both calculation schemes is favorably tested in the non-fractional case, mostly if one takes into account the larger size of the expansion base. Such a difference remains when the RLC problem is solved via diagonalization method, as observed from Fig. 7.

It is noteworthy the fact that, for this problem, fractional descriptions do not seem to largely destroy the symmetry of wavefunctions, when compared to the non-fractional situation. At least, this is true for the lowest allowed states, as seen in Fig. 8. What one may observe in this case is a spatial shift of the entire RLC function profile with respect to conformable one, with further separation when fractionality is greater.

TABLE I. Calculated energy levels (in eV) for the quantum harmonic oscillator with $\hbar\omega = 30$ eV. Results include the exact values for the non-fractional problem, together with the outcome of the analytical WKB solution within Riemann-Liouville formulation and the numerical output of the diagonalization approach (with $N = 500$) to the conformable problem.

Level	Exact	RLC-WKB			Conformable		
	2α	2α			2α		
	2.0	2.0	1.99	1.98	2.0	1.99	1.98
0	15.0	15.000	15.1479	15.2973	14.9978	15.4276	15.8256
1	45.0	45.000	44.2924	45.5862	44.9954	46.2054	47.315
2	75.0	75.000	75.2861	75.5721	74.9573	76.9060	78.6510

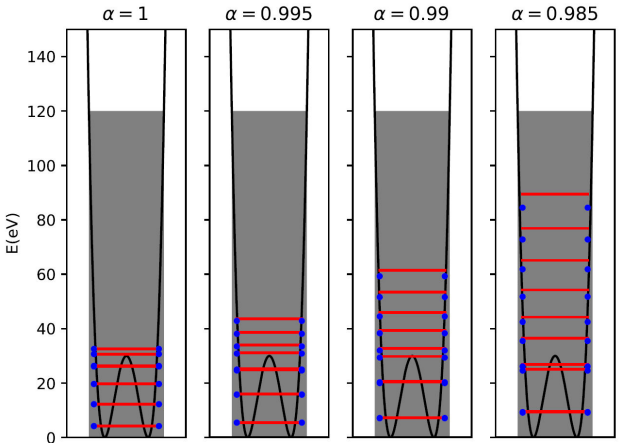

FIGURE 9. The same as in Fig. 7 but for the double parabolic quantum well.

The relevance of the double quantum well problem in quantum mechanics has been widely discussed. Among the related reports one may refer the work in Ref. [17]. The use of this potential function with a parabolic shape in the investigation of semiconductor nanostructures finds recent publication in Refs. [18,19].

In our case, the potential of the double parabolic well is described via the function $V(x) = v_0\left[(x-L/2)^2 - b^2\right]/b^4$. We use the following values for the involved parameters: $v_0 = 30$ eV; $b = 2.5$ nm; $L = 10$ nm. Figure 9 contains calculated energy levels, evaluated via the diagonalization process with $N = 300$. Results appear for both conformable and RLC fractional formalisms. The progressive departure between the level values arising from each of the formulations is also noticed. At the same time, the already commented absence of a defined parity and the switch of probability density local maxima -in excited levels- for the corresponding wavefunctions manifests quite strongly in this problem, as observed from Fig. 10.

At this point, it is worth commenting on some general aspects related to the solution of fractional 1D quantum problems discussed in this work. One of the more prominent

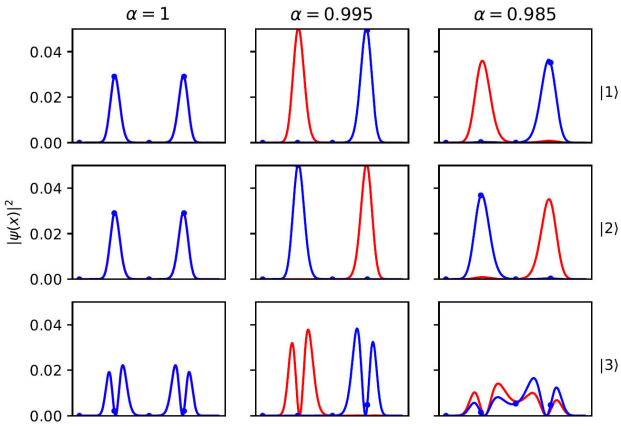

FIGURE 10. The same as in Fig. 8 but for the double parabolic quantum well.

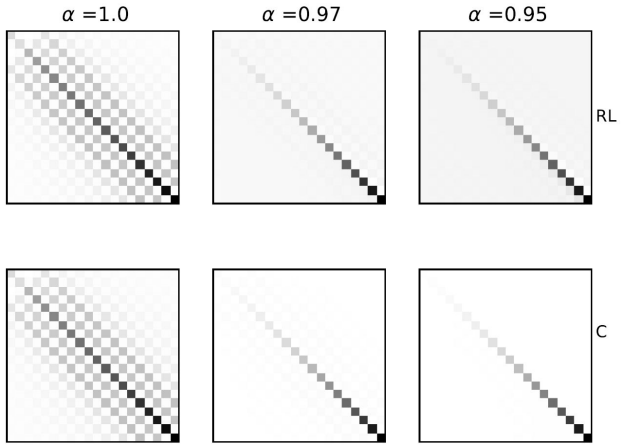

FIGURE 11. Visual representation of the central part of the Hamiltonian matrix for both representation of the fractional differential operator Riemann-Liouville-Caputo (RL) and (C) conformable. Three values of α are considered.

features that distinguish fractional and regular Schrödinger formalisms is the lifting of allowed energy levels in the fractional case, compared to the non-fractional one. As commented, this resembles the effect of narrowing the quantum well width, keeping its depth; but without actual modification of the potential profile geometry. This kind of phenomenon, associated to fractionality, could be of interest in modeling regular quantum phenomena by suitable fitting of an equivalent fractional kinetic energy operator, just as it was made in Ref. [6].

On the other hand, the quantitative differences highlighted throughout this work between results on quantum states in 1D problems, obtained using two distinct fractional formalisms, do not seem to be -only- a consequence of numerical inaccuracies. In fact, the very definition of fractional derivation may have a non negligible influence. This is something that can be better noticed by observing the very elements of both expansion bases, as detailed in the Appendices B and C. Figure 11 displays a visual representation of the near-diagonal part of the Hamiltonian matrix for both representations of the fractional differential operator considered in this work. Again, three values of α are taken, including unity. As noticed, results for both representations have the same form. However, as α decreases, the quantitative weight of Hamiltonian matrix elements around the diagonal changes, as indicated by the behavior of off-diagonal shades of gray. To clarify this issue, Fig. 12 contains a visual matrix form of

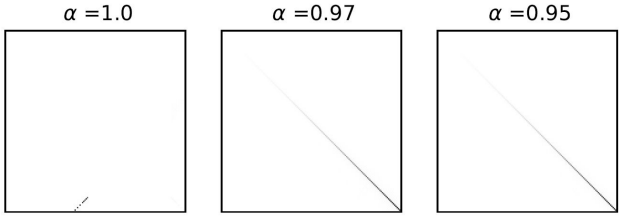

FIGURE 12. Visual representation of the $H_{RL}S_{RL}^{-1} - H_C S_C^{-1}$ considering three values of α.

the difference $H_{RL}S_{RL}^{-1} - H_C S_C^{-1}$, for three values of α. In the latter expression, S_{RL} (S_C) represents the diagonal matrix containing the inner products between basis wavefunctions for the Riemann-Liouville-Caputo (conformable) formulation. In the case of $\alpha = 1$, we observe that all diagonal elements and their respective off-diagonal near ones are in white, which means there are no differences between the two representations, as expected. However, as α decreases, the last diagonal elements of the defined matrix difference take a black shade, suggesting a considerable quantitative separation between these them, which generally contributed to the highest energies, confirming our observation that both representations have differences for high values of energies.

4. Conclusions

We have made a comparison of energy spectra in some one-dimensional quantum mechanical problems addressed within the framework of fractional calculus. In the Schrödinger equation, the kinetic energy operator has been written using fractional derivatives in two different formulations: Conformable and Riemann-Liouville ones.

Illustrative examples chosen are: the single -finite-barrier- quantum well, the double quantum well of finite depth, and the single and double quantum harmonic oscillators. For the first one, besides numerical treatments, based on diagonalization method, analytic solution is provided.

It has been shown that even small deviations -by few percent)-away from integer (non-fractional) formalism would lead to noticeable variations in the values of allowed energy levels. These differences are also noticed when comparing the outcome from both fractional formulations. Besides, in the case of finite barrier systems, the increase in fractionality implies a strong reduction in the number of confined quantum states in the system.

This work has had the main purpose of illustrating on the particularities of fractional quantum mechanics through some of the simplest examples.

Appendix

A. Fractional Rydberg and Bohr radius

Atomic units are often used to convert the quantum equations of motion into dimensionless structures. As initially defined, Rydberg energy is that of an electron in the lowest orbit of Hydrogen atom, whereas the Bohr radius is, precisely, the distance between the nucleus and that very first orbit. In the fractional description, Laskin provides the following definitions [4], respectively:

$$R_{y_\alpha} = (2\alpha - 1)\left(\frac{(e^2)^{2\alpha}}{(2\alpha)^{2\alpha}\mathcal{D}_\alpha}\right)^{\frac{1}{2\alpha-1}}, \qquad \text{(A.1)}$$

where $\mathcal{D}_\alpha = (\hbar^{2\alpha}/2m)(mc)^{2-2\alpha}$, with $0 < \alpha \leq 1$

$$a_0 = \left(\frac{2\alpha\mathcal{D}_\alpha}{e^2}\right)^{\frac{1}{2\alpha-1}}. \qquad \text{(A.2)}$$

Clearly, defining fractional atomic units for each value of α leads to different energy and length scales. For instance, in the case of finite barrier quantum wells, this implies a change in both the spectrum of energy levels and their associated wavefunctions, as noticed from Figs. 1 and 2 in the main text.

B. Diagonalization method: Conformable representation

Let $\phi_n(x) = \sin([n\pi/L^\alpha]x^\alpha)$ to be the elements of an orthogonal base. They are solutions of the fractional problem corresponding to an infinite barrier quantum well of width equal to $2L$, with L being sufficiently larger than the width of the active finite barrier quantum well region (which is assumed to be placed within). Orthogonality is ensured thanks to the Hermitian nature of the operator [15,20]. So that, the wavefunction of the system can be written as the following expansion:

$$\psi(x) = \sum_{n=0}^{N} C_n \sin\left(\frac{n\pi}{L^\alpha}x^\alpha\right). \qquad \text{(B.1)}$$

Then, it is inserted into Eq. (8) to produce

$$\begin{aligned} -\frac{1}{2\alpha-1}\sum_{n=0}^{N} D_x^{2\alpha} C_n \sin\left(\frac{n\pi}{L^\alpha}x^\alpha\right) \\ + \tilde{V}(x)\sum_{n=0}^{N} C_n \sin\left(\frac{n\pi}{L^\alpha}x^\alpha\right) \\ = \tilde{E}\sum_{n=0}^{N} C_n \sin\left(\frac{n\pi}{L^\alpha}x^\alpha\right). \end{aligned} \qquad \text{(B.2)}$$

We take into account the fundamental definition $T_\alpha(f)(t) = t^{1-\alpha}(df/dt)(t)$. Accordingly,

$$T_\alpha\left(\sin\left[\frac{n\pi}{L^\alpha}x^\alpha\right]\right) = x^{1-\alpha}\frac{d\left(\sin\left[\frac{n\pi}{L^\alpha}x^\alpha\right]\right)}{dx}, \qquad \text{(B.3)}$$

$$T_\alpha\left(\sin\left[\frac{n\pi}{L^\alpha}x^\alpha\right]\right) = \alpha\frac{n\pi}{L^\alpha}\left(\cos\left(\frac{n\pi}{L^\alpha}x^\alpha\right]\right). \qquad \text{(B.4)}$$

Now,

$$T_\alpha(T_\alpha(\phi_n)(x)) = T_\alpha\left(\alpha\frac{n\pi}{L^\alpha}\left[\cos\left\{\frac{n\pi}{L^\alpha}x^\alpha\right\}\right]\right), \qquad \text{(B.5)}$$

and, therefore

$$T_\alpha(T_\alpha\alpha(\phi_n)(x)) = -\left(\alpha\frac{n\pi}{L^\alpha}\right)^2\left(\sin\left[\frac{n\pi}{L^\alpha}x^\alpha\right]\right). \qquad \text{(B.6)}$$

As usual, after substitution, the resulting expression is multiplied on both sides by the m-th element of the base. Then, integrating with normalizing weight equal to $x^{\alpha-1}$ [11], one obtains a matrix equation of the form:

$$\frac{1}{2\alpha-1}\sum_{n=0}^{N}\left(\frac{n\pi}{L^{\alpha}}\right)^{2}C_n\int_0^{2L}\sin\left(\frac{m\pi}{L^{\alpha}}x^{\alpha}\right)\sin\left(\frac{n\pi}{L^{\alpha}}x^{\alpha}\right)x^{\alpha-1}dx$$
$$+\sum_{n=0}^{N}C_n\int_0^{2L}\tilde{V}(x)\sin\left(\frac{n\pi}{L^{\alpha}}x^{\alpha}\right)\sin\left(\frac{m\pi}{L^{\alpha}}x^{\alpha}\right)x^{\alpha-1}dx=\tilde{E}\sum_{n=0}^{N}C_n\int_0^{2L}\sin\left(\frac{n\pi}{L^{\alpha}}x^{\alpha}\right)\sin\left(\frac{m\pi}{L^{\alpha}}x^{\alpha}\right)x^{\alpha-1}dx, \quad \text{(B.7)}$$

that, following a diagonalization process, leads to the energy eigenvalues and corresponding wave functions for the one-dimensional quantum problem considered. Unfortunately, regular integration including base functions $\phi_n(x)$ can not be analytically performed, and numerical integration is needed in any case.

C. Diagonalization method: Riemann-Liouville representation

Following Laskin, the orthogonal base in this case can be taken to be: $\phi_n(x)=\sin(n\pi/Lx)$ [2]. In this case, the formulation allows for x to run over the whole real line. So, the enclosing infinite quantum well profile can be extended within $[-L,\,L]$ (and, also, the active region can be taken to be symmetric with respect to the origin). Besides, the definition of the inner product includes a weight equal to unity. Under these conditions, the expansion for the wavefunction will be:

$$\psi(x)=\sum_{n=0}^{N}C_n\sin\left(\frac{n\pi}{L}x\right). \quad \text{(C.1)}$$

By substituting this solution in Eq. (8), one gets

$$-\frac{1}{2\alpha-1}\sum_{n=0}^{N}D_x^{2\alpha}C_n\sin\left(\frac{n\pi}{L}x\right)+\tilde{V}(x)\sum_{n=0}^{N}C_n\sin\left(\frac{n\pi}{L}x\right)=\tilde{E}\sum_{n=0}^{N}C_n\sin\left(\frac{n\pi}{L}x\right). \quad \text{(C.2)}$$

Now, multiplying by another element of the same base, say, $\sin([m\pi/L]x)$ and integrating, one finds;

$$-\frac{1}{2\alpha-1}\sum_{n=0}^{N}C_n\int_{-L}^{L}\sin\left(\frac{m\pi}{L}x\right)D_x^{2\alpha}\sin\left(\frac{n\pi}{L}x\right)dx$$
$$+\sum_{n=0}^{N}C_n\int_{-L}^{L}\tilde{V}(x)\sin\left(\frac{m\pi}{L}x\right)\sin\left(\frac{n\pi}{L}x\right)dx=\tilde{E}\sum_{n=0}^{N}C_n\int_{-L}^{L}\sin\left(\frac{m\pi}{L}x\right)\sin\left(\frac{n\pi}{L}x\right)dx. \quad \text{(C.3)}$$

With the use of the RLC formulation of the fractional derivative:

$${}_{\infty}D_{RLC}^{\alpha}\sin(\lambda r)=\lambda^{\alpha}\sin\left(\lambda r+\frac{\alpha\pi}{2}\right). \quad \text{(C.4)}$$

That is;

$$D_x^{2\alpha}\sin\left(\frac{n\pi}{L}x\right)=\left(\frac{n\pi}{L}\right)^{2\alpha}\sin\left(\frac{n\pi}{L}x+\pi\alpha\right), \quad \text{(C.5)}$$

finally obtaining:

$$-\frac{1}{2\alpha-1}\sum_{n=0}^{N}C_n\left(\frac{n\pi}{L}\right)^{2\alpha}\int_{-L}^{L}\sin\left(\frac{m\pi}{L}x\right)\sin\left(\frac{n\pi}{L}x+\pi\alpha\right)dx$$
$$+\sum_{n=0}^{N}C_n\int_{-L}^{L}\tilde{V}(x)\sin\left(\frac{m\pi}{L}x\right)\sin\left(\frac{n\pi}{L}x\right)dx=\tilde{E}\sum_{n=0}^{N}C_n\int_{-L}^{L}\sin\left(\frac{m\pi}{L}x\right)\sin\left(\frac{n\pi}{L}x\right)dx. \quad \text{(C.6)}$$

Acknowledgments

MEMR is grateful to Mexican CONAHCYT for support through Grant CB 2017-2018 No. A1-S-8218.

1. I. Podlubny, Fractional Differential Equations: An Introduction to Fractional Derivatives, Fractional Differential Equations, to Methods of their Solution and some of their Applications (Mathematics in Science and Engineering, Academic Press, San Diego, USA, 1998).
2. N. Laskin, Fractals and quantum mechanics, *Chaos: An Interdisciplinary Journal of Nonlinear Science* **10** (2000) 780, https://doi.org/10.1063/1.1050284.
3. N. Laskin, Fractional Schrödinger equation, *Phys. Rev. E* **66** (2002) 056108, https://doi.org/10.1103/PhysRevE.66.056108.
4. N. Laskin, Fractional quantum mechanics, *Phys. Rev. E* **62** (2000) 3135, https://doi.org/10.1103/PhysRevE.62.3135.
5. J. Dong and M. Xu, Some solutions to the space fractional Schrödinger equation using momentum representation method, *J. Math. Phys.* **48** (2007) 072105, https://doi.org/10.1063/1.2749172.
6. L. Y. Medina, F. Núñez-Zarur, and J. F. Pérez-Torres, Nonadiabatic effects in the nuclear probability and flux densities through the fractional Schrödinger equation, *International Journal of Quantum Chemistry* **119** (2019) e25952. https://doi.org/10.1002/qua.25952.
7. R. Khalil *et al*., A new definition of fractional derivative, *Journal of Computational and Applied Mathematics* **264** (2014) 65, https://doi.org/10.1016/j.cam.2014.01.002.
8. W. S. Chung, Fractional Newton mechanics with conformable fractional derivative, *Journal of Computational and Applied Mathematics* **290** (2015) 150, https://doi.org/10.1016/j.cam.2015.04.049.
9. M. K. A. Kaabar *et al*., Novel Investigation of Multivariable Conformable Calculus for Modeling Scientific Phenomena, *Journal of Mathematics* **2021** (2021) 3670176, https://doi.org/10.1155/2021/3670176.
10. N. Korichi, A. Boumali, and H. Hassanabadi, Thermal properties of the one-dimensional space quantum fractional Dirac Oscillator, *Physica A: Statistical Mechanics and its Applications* **587** (2022) 126508, https://doi.org/10.1016/j.physa.2021.126508.
11. W. S. Chung *et al*., The effect of fractional calculus on the formation of quantum-mechanical operators, *Mathematical Methods in the Applied Sciences* **43** (2020) 6950, https://doi.org/10.1002/mma.6445.
12. E. M. Rabei, M. Al-Masaeed, and A. Al-Jamel, Solution of the Conformable Angular Equation of the Schrödinger Equation, arXiv:2203.11615 [quantph], https://doi.org/10.48550/arXiv.2203.11615.
13. E. O. Odoh and A. S. Njapba, A review of semiconductor quantum well devices, *Advances in Physics Theories and Applications* **46** (2015) 26.
14. N. Grandjean, B. Damilano, and J. Massies, Group-III nitride quantum heterostructures grown by molecular beam epitaxy, *Journal of Physics: Condensed Matter* **13** (2001) 6945, https://doi.org/10.1088/0953-8984/13/32/305.
15. Y. Wei, The Infinite Square Well Problem in the Standard, Fractional, and Relativistic Quantum Mechanics, *International Journal of Theoretical and Mathematical Physics* **5** (2015) 58, https://doi.org/10.5923/j.ijtmp.20150504.02.
16. R. Hermann, Infrared spectroscopy of diatomic molecules a fractional calculus approach, *International Journal of Modern Physics B* **27** (2013) 1350019, https://doi.org/10.1142/S0217979213500197.
17. V. Jelic and F. Marsiglio, The double-well potential in quantum mechanics: a simple, numerically exact formulation, *European Journal of Physics* **33** (2012) 1651, https://doi.org/10.1088/0143-0807/33/6/1651.
18. S.-F. Ma, Y. Qu, and S.-L. Ban, Intersubband optical absorption of electrons in double parabolic quantum wells of AlxGa1-xAs/AlyGa1-yAs, *Chinese Physics B* **27** (2018) 027103, https://doi.org/10.1088/1674-1056/27/2/027103.
19. E. Kasapoglu, M. B. Yücel, and C. A. Duque, Parabolic Gaussian Double Quantum Wells under a Nonresonant Intense Laser Field, *Nanomaterials* **13** (2023) 1360, https://doi.org/10.3390/nano13081360.
20. E. V. Kirichenko *et al*., Lévy flights in an infinite potential well as a hypersingular Fredholm problem., *Physical Review E* **93** (2016) 052110, https://doi.org/10.1103/PhysRevE.93.052110.
21. Y. Wei, Comment on Fractional quantum mechanics and Fractional Schrödinger equation, *Phys. Rev. E* **93** (2016) 066103, https://doi.org/10.1103/PhysRevE.93.066103.
22. R. Khalil and H. Abu-Shaab, Solution of some conformable fractional deferenctial equations, *International J. Pure and Applied Math.* **103** (2015) 667, http://dx.doi.org/10.12732/ijpam.v103i4.6.